BULLETIN OF THE EARTHQUAKE
RESEARCH INSTITUTE
Vol. 38 (1960), pp. 241-254

14. *The Observation of Microseisms at a Wave Gauge Station. —On the Origin of Microseisms (Part III).—*

By Tetsuo A. SANTÔ,

Earthquake Research Institute.

(Read Nov. 24, 1959.—Received March 28, 1960)

1. Introduction

In Part I[1], the writer made an investigation into the features of microseismic occurrence due to the passing of a single cyclone, a typhoon or a strong cold front, using many observational data at many stations in Japan.

The most important feature was that when a cyclone or a typhoon is travelling towards northeast over the ocean, the microseismic storm shifts from one region to another as if running after the cyclonic center, and further, the largest microseismic storm at a given station occurs considerably later than the passing of a cyclonic center. This feature was quite conspicuous for northern stations, when the travelling speed of cyclonic center had become very high.

This phenomenon is quite similar to the arriving of the water wave pattern caused by a single vibrating source which runs over the water with a velocity higher than the group velocity of the water wave.

Not a few authors[2] found the fact that a microseismic storm at a certain station becomes heaviest after the passing of a cyclonic center offshore, but this feature was reported only as an observational fact, and has never been explained. For the present author, however, this fact seems to be very important in order to explain the origin of microseisms. That is the problem of where the energy of the swell turns to microseismic waves.

1) T. A. SANTÔ, "Investigations into Microseisms Using the Observational Data of Many Stations in Japan (Part I).—On the Origin of Microseisms.—", *Bull. Earthq. Res. Inst.*, **37** (1959), 307.

2) For instance, F. I. MONAKHOV, "Development of Microseismic Method of Tracing Storms at Sea," *Abstracts of the Reports at the XI General Assembly of the International Union of Geodesy and Geophysics* (1957), 76.

In paper II[3], this phenomenon was further investigated adding the data of microseismic storms due to the passing of many typhoons. The method was to check the relation between V and L/D measuring the three values V (the travelling speed of a cyclonic center), D (the shortest distance from a coast near a station to the travelling course of a cyclone), and L ($=Vt$, in which t means the "delayed time") on a map. (See Fig. 2a)

This was examined and the approximate linear relation between V and L/D was observed.

2. The "eye of a microseismic storm" around the cyclonic center

The nature of the occurrence of microseismic storms due to the passing of a cyclone or a typhoon can be explained more clearly as follows, if we examine the relation between D and L/V instead of V and L/D.

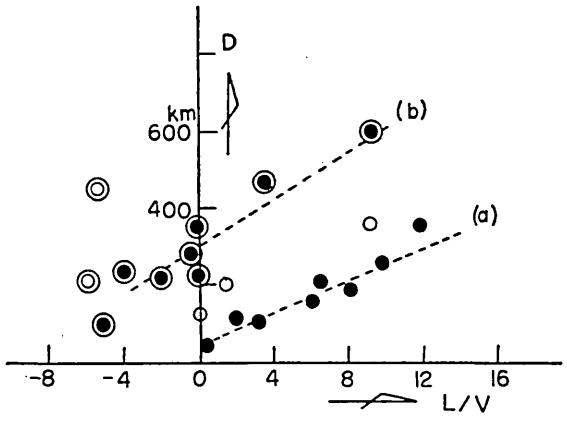

Fig. 1. Observed relation for $D-L/V$. Black and double black circles correspond to the cyclones with $p_0>1000$ mb. and with $p_0<985$ mb. respectively. White and double white circles are for the cases when cyclonic centers ($p_0>1000$ mb. and $p_0<985$ mb. respectively) passed at the left side of the station.

The relation between D and L/V is given in Fig. 1. From this figure we can recognize that the data for the cyclones of $p_0>1000$ mb. (black circles) and for those of $p_0<985$ mb. (double black circles) distribute around the two straight lines, which can be expressed as

$$D=v(p_0)(L/V)+D_0(p_0). \quad (1)$$

In this figure, the white circles (for $p_0>1000$ mb.) and double white circles (for $p_0<985$ mb.) show the data for the cases when cyclonic centers passed on the left side of the station.

3) T. A. SANTÔ, "Investigations into Microseisms by the Observational Data of Many Stations (Part II).—Further Considerations on the Origin of Microseisms.—". *Bull. Earthq. Res. Inst.*, **37** (1959), 483.

The above equation (1) can be explained as follows.

Suppose a region which is enveloped by a curve C around a cyclonic center (Fig. 2b) and the highest swells which arrived at some coast near the station had been sent out from this boundary. Then,

$$D'=D-D_0=vt' \qquad \text{and} \qquad L=Vt' , \qquad (2)$$

in which t' mean the travel time of the swell which cover the distance D'. From these equations,

$$(D-D_0)/v=L/V$$

From this, we can reduce the same equation as (1), namely,

$$D=v(L/V)+D_0$$

Therefore, D_0 on the right hand of the equation (1) means the radius of the assumed region towards the station. Further, our observed results concerning the relation between D and L/V tell that the heaviest microseismic storm occurs at the time when the highest swell which had started from the boundary C reaches some coast near the station. For this reason, this enveloped region around a cyclonic center can be called "the eye of the microseismic storm".

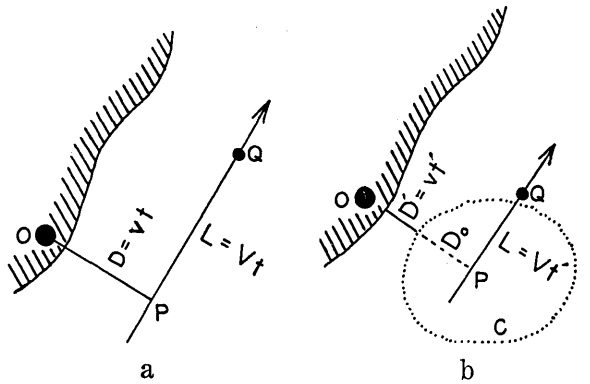

Fig. 2a. Schematic figure which shows the relation between L and D for the case of a single point source travelling over the water with the velocity V which is greater than the group velocity of water waves v.

Fig. 2b. Assumed envelope curve C (dotted line) around a cyclonic center.

The values of v estimated from the inclinations of these lines are approximately 20 km/hr and 30 km/hr respectively, which are reasonable for the velocities of swells belonging to the cyclones with these central pressure ranges. The radius (D_0) of the enveloped region can be read by the intercept points of these straight lines at the D axis. They are read as approximately several tens kilometers from the line (a) (for $p_0>1000$ mb.) and as few hundreds kilometers from the line (b) (for $p_0<985$ mb.) re-

spectively. It must be noticed in the same figure that D_0 was estimated somewhat larger for the data represented by white and double white circles. It means that the envelope curve swells to the right for travelling directions of cyclones as is shown in the schematic figures of 2b. This result is also quite reasonable. For, as is well known, the energy of a cyclone is, in the northern Hemisphere, stronger on the right side of its travelling direction.

In equation (1), when $D=D_0$, L becomes 0, that is, when a cyclone passed offshore so near as to contact the "eye of the microseismic storm" C on the coast (Fig. 3a), the microseismic storm becomes largest at the time when the cyclonic center passes offshore near the coast.

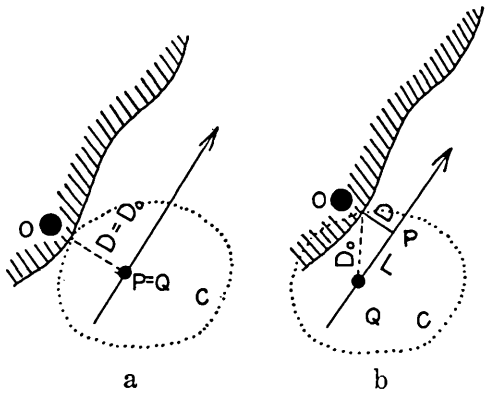

Fig. 3a. Schematic figure which shows the position of a cyclone when it passes offshore near the coast with the distance equal to D_0.

Fig. 3b. Schematic figure which shows the relation between D and L when a cyclonic center passes offshore near the coast so near as $D<D_0$.

Further, when $D<D_0$, L becomes minus (See Fig. 3b). It means that when a cyclone passes much nearer the coast as the "eye" enters into the land, the heaviest microseismic storm occurs earlier than the passing of the cyclone offshore. As was found before, D_0 is larger for smaller values of p_0. Therefore, when p_0 is very small, the circumstances which satisfy the condition $D<D_0$ occur more frequently. They were thecases for the southern stations in Japan, around which typhoons are generally still quite strong. (All of the data of minus side of L/V axis in Fig. 1 correspond to the data obtained at southern stations.)

In this case, as is shown in Fig. 3b,

$$D_0=\sqrt{D^2+L^2}\,. \qquad (3)$$

By this equation (when $L<0$) and by the equation (1) (when $L\geqq 0$), we can again estimate the values of D_0 by using the data of L, V and D of each case. In these estimations, v were calculated by the equation $v=gT/4\pi$, in which g and T mean the acceleration due to gravity and

the period of swells respectively[4]. The results are shown in Fig. 4. In this figure, the marks are all the same with those used in Fig. 1. The expected tendency that D_0 will be a decreasing function of p_0 can be seen in this figure although the points are scattered because of the difference of the meteorological conditions around the cyclonic center. The values of D_0 thus estimated are approximately equal to the previous ones. Moreover, it can also be seen that the values of D_0 determined by the white and double white circles are larger than by the others. It means, as we expected, that the "eye" swells to the right in the course of its travel as is shown in the schematic figure of 3.

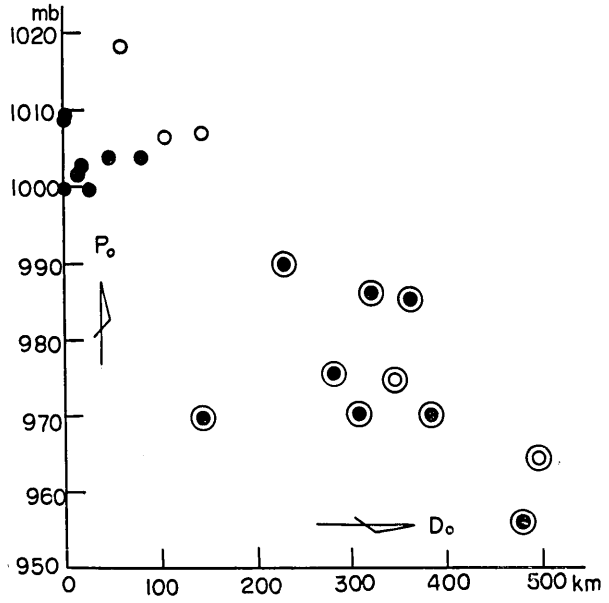

Fig. 4. Values of D_0 estimated by the equation $D_0 = D - v(L/V)$ when $L \geqq 0$, and by the equation $D_0 = \sqrt{D^2 + L^2}$ when $L < 0$ respectively.

In any case, it became clear that the largest microseismic storm due to the passing of cyclones or typhoons occurs at the time when the highest swell reaches some part of the coast near the stations.

In order to make this conclusion clearer, the direct method was taken. Namely, the simultaneity between the occurrence of the largest microseismic storm and the arriving of the highest swells at the same station was examined.

3. The position and the method

Microseismic observation began from September, 1959 at one of the wave gauge stations Naarai, approximately 100 km east of Tokyo and situated nearly at the top of the Inubô Promontory (Fig. 5). In Fig. 5,

4) S. UNOKI, "On the Speed, Travel Time and Direction of Ocean Waves due to Tropical Cyclones," *Journ. Met. Soc. Japan*, **34**, 2, (1956), 354.

the wave gauge and the seismograph station are shown respectively by S and O.

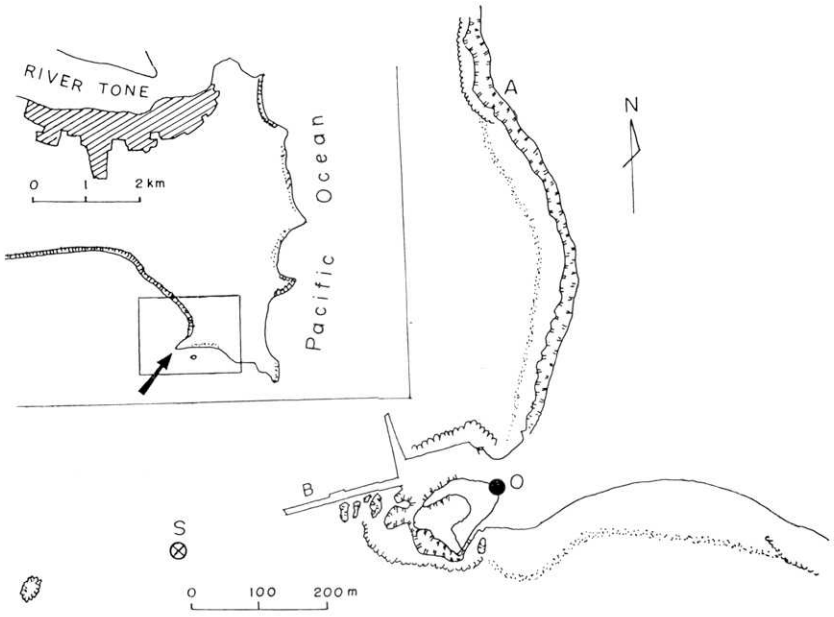

Fig. 5. The map which shows the positions of microseismic observations (O) and of wave gauge (S) respectively. The location of this wave gauge stations Naarai is shown in the annexed small map.

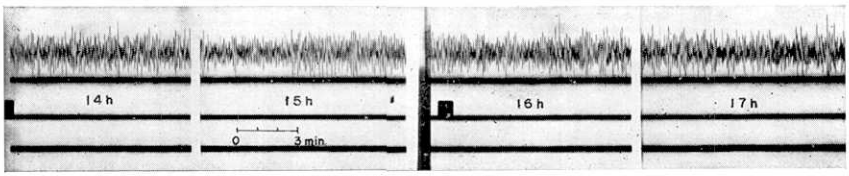

T-5919, OCT. 21^{d} 14^{h}~17^{h}

Fig. 6. An example of microseismic records obtained by slow speed recording camera.

As the purpose of the present work is to find out the times when microseismic amplitudes become largest, and to compare them with those of swells, the running speed of the recording camera of the seismograph was slowed down to as little as 1 cm/min. The recording mechanism was so designed as to start at 00 minutes, continue to work 10 minutes and then stop automatically. A sample of the records thus obtained is shown in Fig. 6.

4. The results

The results of time variations between M (the microseismic amplitudes) and S (swell heights) due to the passing of five typhoons 5914, 5915, 5916, 5918 and 5919 are shown in Fig. 7. In this figure, other data W (the wind velocity measured at the same station Naarai), D (the distance of cyclonic center from Naarai) and p_0 (central pressure) are also shown for reference. The vertical broken lines show the time

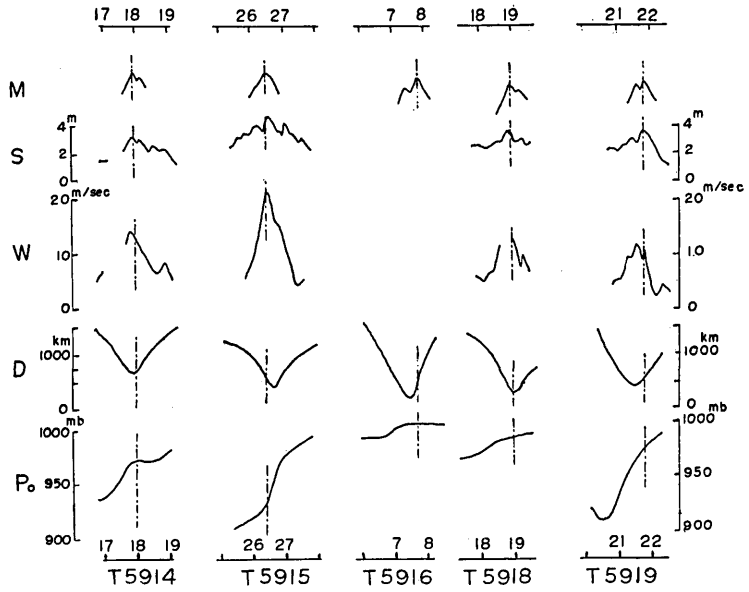

Fig. 7. Variations of microseismic amplitudes (M), swell heights (S), wind velocities (W) at Naarai due to the passing of typhoons. Variations of distances (D) from the cyclonic centers to the station and of central pressure (p_0) are also shown.

when M reached maximum. This figure shows the remarkable correlation between the growth and decay of M and S. However, since the difference between the times of M_{max} and S_{max} is not clear on too narrow a times scale, another representation was taken in Fig. 8, in which the times of M_{max}, S_{max} and W_{max} are shown by three kinds of arrows on every travelling path of typhoon. Seeing this figure, the times of M_{max} and S_{max} seem to be slightly different. But we need not expect them to coincide exactly. For, the standing wave of swells cannot be caused just at the wave gauge station S. From the topographical features

around Naarai (See Fig. 5), the coast along the steep cliff beyond "A" may be one of the suitable region where a standing sea wave occurs due to the interference between the incident and reflected waves. If this assumption is the case and microseismic amplitudes were mainly effected by this origin, the times of M_{max} will be measured about forty or fifty minutes later than those of S_{max}. (The swells were always coming from the south).

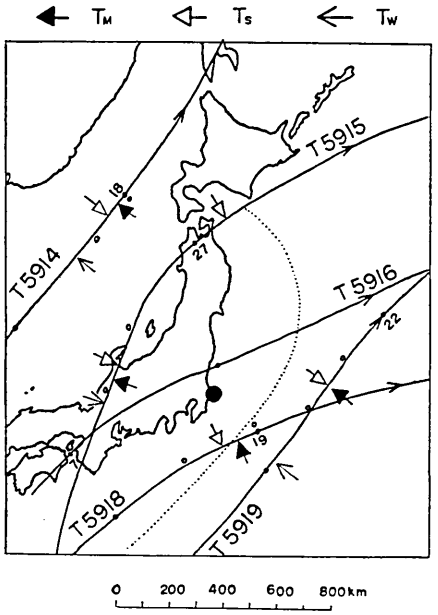

Fig. 8. Travelling paths of typhoons. The different arrows on each path show the times of T_M (when the maximum microseismic amplitudes were recorded), T_S (when the highest swells were recorded), and T_W (when the largest wind velocity were recorded). Small circles mean the recording times of swells before and after the T_S.

Further, considering that the observations of swells were made for twenty minutes every two hours (The two observation times before and after the times of S_{max} are marked by small white circles in Fig. 8.), we can conclude from these results that the microseismic storm became largest nearly at the time when the highest swell reached some part of the coast near the station without regard to the position and the movement of the cyclonic center.

On the case of the typhoon 5915, we can see in Fig. 8 the second maximum of the swell heights which occurred at 27 d 01 h. (Regrettable to say, the recording of microseisms had already been stopped by this time.) Examining the weather map around that time, it was found that this cyclonic center (typhoon 5915 had already weakened and had changed into a cyclone) was followed by a strong cold front (dotted lines in Fig. 8) which was just entering into the Pacific Ocean. Remembering here the feature that microseismic storms in Japan become heaviest due to the same circumstances[5], we can guess from this fact also that the heaviest microseismic storm occurred at the same time.

There is another fact to be noticed. That is, even in such a case as that of typhoon 5914 which travelled through the Japan Sea, the

5) *loc. cit.* (1).

microseisms at Naarai were greatly influenced by the swells on the Pacific Ocean. Since the microseismic storm region due to the passing of a single cyclonic center is not large in Japan (See Fig. 3 or Fig. 5 in Part I), we can conclude that the microseisms at a certain station are mostly influenced by the swells near the station.

It was firstly noticed by B. Gutenberg that microseisms can propagate for a great distance over the continental path with a uniform structure, but they suffer marked attenuation in geologically disturbed areas. In Japan, microseisms show, as is stated above, rather large attenuation, which may be due to the disturbed structure of the Island.

5. On the periods of Microseisms

The relation between the periods of microseisms (*Pm*) and that of swells (*Ps*) measured at the same time and nearly the same position has often been studied by many authors, and it is well known that *Pm* is approximately equal to the half of *Ps*. The present author also found the same relation and it was reported in the first paper. By these facts and by the experimental study done by R.I.B. Cooper and M. S. Longuet-Higgins[6], the standing wave theory theoretically established by Higgins[7] has become the most powerful one to explain the mechanism of the generation of microseisms.

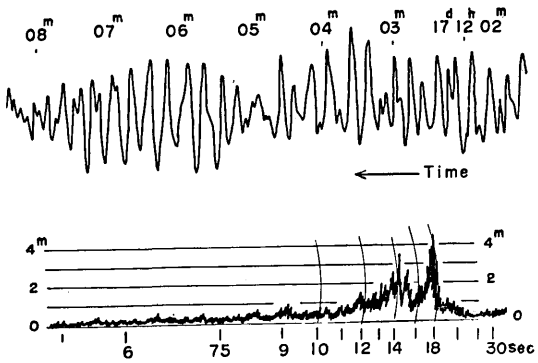

Fig. 9. Wave form of swells recorded at Naarai at the passing of the typhoon 5821 (above), and the corresponding period spectrum (below).

However, before we adopt his theory to explain the period relation above stated, we must clear up the doubt whether the swells contained second harmonic waves and whether the instruments for microseisms having a good respone from four to seven seconds predominantly recorded

6) M. S. LONGUET-HIGGINS and R. I. B. COOPER, "An Experimental Study of the Pressure Variations in Standing Water Waves," *Proc. Roy. Soc. A*, **206** (1951), 424.

7) M. S. LONGUET-HIGGINS, "A Theory of the Origin of Microseisms," *Phil. Trans. Roy. Soc. London, A*, **243** (1950), 1.

such second harmonic waves.

Recently, a spectrum computor "MERIAC-I-F" has been completed at the Oceanographical Laboratory, Meteorological Research Institute, Tokyo[8]. The period spectrum of swell at Naarai were obtained by this computor. An example of the wave form of swells and the corresponding spectrum are given in Fig. 9. As is well recognized in this example, the spectrum of swells does not contain any noticeable second harmonics. Therefore, in order to explain the relation of $Pm=\frac{1}{2}Ps$, we have to adopt the standing wave theory.

6. Some experimental observations

Occasionally, running speed of the recording paper was increased in order to see the fine structure of a wave. Fig. 10 shows some examples thus obtained, in which the upper two records (A) are those by two horizontal seismographs both installed in NS direction in order

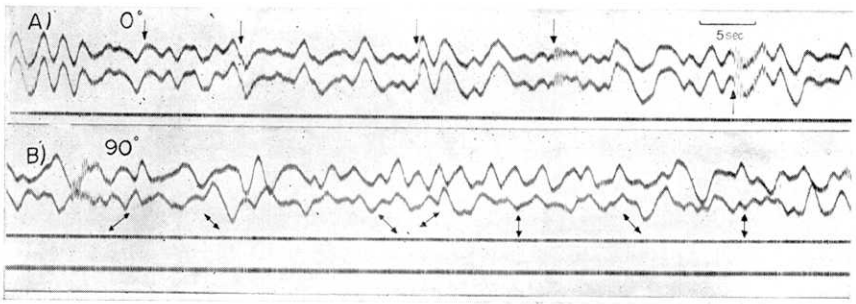

Fig. 10. An examples of the wave form of microseisms at Naarai. A) is obtained by two horizontal seismographs both installed in NS direction in order to check the similarity of their characteristics. Several arrows mean the shock waves due to the collisions of swells at the breakwater B which is approximately 200 m apart from the observational position (see Fig. 5). In B), the lower wave form was obtained by turning one of the seismographs in EW direction. Arrows show the direction of ground motion estimated by the phase relation between the two records.

to check the similarity of their characteristics, while in the lower two (B), one of the seismograph was turned to EW direction.

As will be recognized in Fig. 5, observational point O is surrounded by intricate cliffs or many small rocky islands near the coast. Beside

8) T. FURUHATA, "Atarashii Zidô Dêta Syorikikai MERIAC-1-F ni Tsuite", (in Japanese), *Kisyô to Tôkei*, **10** (1959), 23.

the two breakwaters, many concrete blocks which will be used to build a new breakwater were piled up here and there in the water. It was observed that many small standing waves took place among and behind these complicated obstacles. For this reason, the recorded microseismic waves were irregular and had rather short periods. In the record (A), we can see small and very short period waves marked by arrows. They are the waves caused by the direct collisions of high swells at the southern side of the breakwater B which projects westward into the Ocean (See Fig. 5). It must be remarked here that the elastic waves due to such direct collisions of swells with the breakwater decrease very rapidly, and do not seem to bring up any long period elastic waves in the earth.

By two records in (B), the directions of ground vibrations due to microseismic waves can be estimated from the phase relations. These are represented by arrows at the corresponding waves. As has been reported by many authors, the propagating directions of microseismic waves are not constant but frequently change at random. In this figure, this nature is also well recognized.

7. Conclusions of this paper and some discussions on the origin of microseisms

1) A new relation was discovered between the position of a cyclonic center, its travelling speed and its central pressure when it causes the largest microseismic storm at a given station. This relation was well explained by supposing an "eye of the microseismic storm" around the cyclonic center from the boundary of which the highest swells for the coast near the station were sent out. The dimensions of the radius of this swelling region were roughly estimated as several tens kilometers for the cyclones ($p_0 > 1000$ mb.) and as few hundreds kilometers for the typhoons ($p_0 < 985$ mb.) respectively.

2) Microseismic observations were made at a gauge station, and it became clearer that the energy of swells changes into microseismic waves at some steep coast. Further, the following facts could be recognized.

a) The direct collisions of swells at steep cliffs cause very short period waves, but these waves show a rapid attenuation and cannot bring up microseismic waves.

b) Sea waves much disturbed among and behind many complicated

obstacles around the station produced rather short period (three to five seconds) local microseisms. As has often been observed usually, these microseismic waves seem to come from diverged directions. The phenomenon observed at Naarai, therefore, looks like a model of usual microseisms.

c) At least in Japan where geological structure is disturbed, the microseismic amplitudes are mostly influenced by the swells near the station.

3) Period spectrum of swells were computed and no noticeable second harmonics were found. By this examination, the standing wave theory was emphasized.

Through the studies from various aspects that have been described in three papers, the writer have reached a final conclusion on the origin of microseisms. Namely, the microseismic waves are generated somewhere at a steep coast where sea waves can be reflected.

By the above conclusion, most of the complicated results which have been reached by observations at one or few stations in a limited district and have made the character of microseisms quite obscure will be clearly explained as follows:

Probably, such microseismic origins are distributed near the observational stations. Especially, stations on an Island are surrounded by many such origins with various strengths according to such conditions as the reflective coefficient of swell at these origins, the length of the steep coast, or the elastic conditions beneath the sea at these origins. (After the experimental study by R. I. B. Cooper and M. S. Longuet-Higgins[9], water waves were reflected by such gentle sloped plate as 20° with the reflective coefficient of 0.32). On the other hand, the heights of swells coming into each origin are not constant but change occasionally and independently. Therefore, when we observe microseismic waves by, for instance, the tripartite method, they look as if they come from various directions at random.

Further, when there is a strong origin somewhere, the microseismic wave from that origin will always be predominant in spite of the shift of energy source (cyclonic center) on the Ocean.

The velocity of microseismic waves cannot be measured unless we can detect the waves which come from one origin. Otherwise, we are apt to measure the apparent velocity which is uncertain.

9) *loc. cit.* (6).

8. Acknowledgements

The writer wishes to express his hearty thanks to Dr. K. Wadati, the Chief of the Japan Meteorological Agency, to Mr. S. Miyamura and to Dr. Y. Satô for their encouragement and guidance during the present studies.

Many thanks are also due to Dr. S. Unoki for his valuable advice from the oceanographical point of view.

The writer is greatly indebted to Mr. T. Kizawa for the collection of swell data.

The writer cannot forget Mr. N. Hoshino and Mr. N. Takagi for their help and kindness during the observations at Naarai.

---

14. 脈 動 源 に つ い て (第 三 報)
——波浪観測点における脈動観測——

地震研究所 三 東 哲 夫

前稿では，ある場所の脈動振巾が最大になつた時の台風や低気圧の速度，位置および中心示度などの間には，ある関係式が成立つことを述べたが，さらに本稿では，まづ低気圧や台風の中心のまわりに，ある領域を考え (第 2b 図) 脈動観測点付近の海岸に最高の波浪として到達する波がこの領域のへりから送り出されたと考えるとうまく説明のつく新しい関係式を導いた (式 (1)). この領域の半径は，低気圧や台風の進行方向の左側では，中心示度が 1000 ミリバール以上の低気圧では数十キロメートル，中心示度が 985 ミリバール位以下の台風では 300～400 キロメートル位のもので，進行方向の右側ではこれ等よりもやや大きい．つまり，さうした領域のふちから出た波浪が，観測点付近の海岸に最高の波浪として到達し，それと同時にそこの脈動が一番大きくなる，ということで，ある場所の脈動と，それをおこすエネルギー源である低気圧や台風の速度や大きさ，およびその位置などに関係した時間的空間的な相互関係がうまく説明されてくる．

そこでつぎには，果してそれならば，ある場所での波浪が一番高くなつた時に，その同じ場所での脈動も同時に一番大きくなるだろうか，という点に関する直接の確証が望まれてくる．そこで今回，千葉県銚子市の名洗港 (第 5 図) で脈動を観測し，その振巾の最大時が同じ場所で運輸省第二港湾建設局の行なつている波浪観測の波高の最大時と果して一致するかどうかを調べて見た．その結果は予想通りであつて，この両者はかなりよく一致した (第 8 図).

さらに，今度の観測で認められたことは，

a) 防波堤に直接打ち当る衝撃力は，脈動にはならないこと (第 10 図の A).

b) 少なくとも日本では，ある場所の脈動振巾は，ほとんどその場所の近くの波浪の高さで左右され，広い範囲にわたつて一様な地殻構造をもつた大陸で従来認められているようには脈動は伝播してゆかないこと．

c) 観測点周囲の複雑に入りこんだ崖や，妨害物等によつて，局部的な定常波が方々で見られたが，脈動による地面の動きも，これ等の局部的な定常波発生源を脈動源と考えて差支えないこと (第 10 図の B).

等である．

また，脈動の周期がいつも波浪の周期の約半分になつているという点を説明する定常波説をより一層確認する目的で，波浪の波形の中には第二高調波がほとんどないことを，最近気象研究所の海洋研究部で完成されたスペクトル分析器による結果で確めた（第 9 図）.

以上三部にわたつて，いろいろの角度から脈動の発生する場所についての究明を試みて来たが，結局帰するところは，脈動は波浪が海岸に到達し，海岸線上のどこか，十分な反射波が生じうる場所で入射波と反射波との間に起る定常波によつて発生する，ということである．このような発生源は，当然それぞれの場所における波浪の反射率の大小，定常波発生領域の広狭，さらには，その領域の海底における弾性波の吸収係数の大小等に左右される「強さ」を一つ一つ持つているであろう．しかも，これ等の異つた強さをもつ発生源の一つ一つからやつてくる脈動波自体が，また一定の振巾ではありえない．何故ならば，それぞれの発生源に送りこまれる波浪の高さ自体が，それぞれ独立に絶えず変動をくり返す性質のものだからである．したがつて，局部的に脈動を観測する限り，脈動波は全く不規則にあちこちからやつてくるように見える．また，特に強い発生源がある方向に存在する場合には，海上をエネルギー源（低気圧や台風）が移動しても，この強い発生源からの脈動波が終始卓越して観測されることも当然ありうる．
